Frequency Domain Block Turbo-Equalization for Single-Carrier Transmission over MIMO Broadband Wireless Channel

Raphaël Visoz, Member IEEE, Antoine O. Berthet , Member IEEE, Sami Chtourou, Student Member IEEE

Abstract

This paper presents a new class of block turbo-equalizers for single-carrier transmission over Multiple-Input Multiple-Output (MIMO) broadband wireless channel. The key underlying idea consists in equalizing (non overlapping) groups of symbols and detecting their individual space-time components in a disjoint and iterative fashion. This functional split naturally induces new design options that have been accurately listed and described, i.e., choice of distinct criteria for InterGroup Interference (IGI) equalization and intra-group components detection, yielding hybrid structures, multiple iterative loops and related scheduling variants. Selected algorithms in the proposed class are compared in terms of performance under various transmission scenarios. For all of them, Minimum Mean Square Error (MMSE) IGI equalization certainly occupies a central role (at least for the first iteration) and may be identified as the computational bottleneck. Fortunately, block spread transmission together with cyclic prefix operations make the channel matrix block circulant, thus allowing low complexity inversion in the Fourier domain.

I. INTRODUCTION

The Generalized Multi-Carrier (GMC) quasi-synchronous Code Division Multiple Access (CDMA) [1] was recently advertised as the framework for future-generation (4G) broadband radio interfaces [2]. This concept relies on three key features, namely block spread transmission (quasi-static channel assumed), cyclic prefix (to suppress InterBlock Interference (IBI) and guarantee channel matrix circularity) and judicious choice of the user signatures (to mitigate other types of interferences). GMC-CDMA allows an unifying formalism which, in particular, encompasses Single-Carrier Transmission with Cyclic Prefix (SCT-CP), seen as a form of Multi-Carrier Transmission (MCT) with Discrete Fourier Transform (DFT) precoding. SCT-CP, the main concern here, is demonstrated to have a twofold interest compared to MCT: it reduces the Peak-to-Average Power Ratio (PAPR), which is crucial for mobile terminals (cheaper power amplifiers and/or greater range for the uplink), and is far less sensitive to phase noise and frequency offsets [3] [4] [5]. Furthermore, SCT-CP efficiently exploits frequency diversity, through the recovery of inherent multipath diversity. Indeed, broadband wireless channels can be turned into equivalent channels with very little small-scale fluctuations via powerful block turbo-equalizers. As a matter of fact, the complexity of such advanced receivers is much higher than the one of typical MC receivers. However, thanks to the CP insertion at the transmitter, their complexity can be drastically reduced by implementing them in the frequency domain (see [7]-[12] and the references therein).

This paper describes a broad family of frequency domain block turbo-equalizers for SCT-CP over MIMO broadband wireless channel. We intentionally focus on Block Linear Equalization (BLTE) at first iteration [6] [8] [10] [13] [14] since, contrary to what asserted in [12, p. 468], it is more efficient for coded systems and less complex than Block Decision-Feedback Equalization (BDFTE) within an iterative structure [14, VIII. Conclusion]. Not only do we content with generalizing [7] to the MIMO case, but we focus our derivations on a recently introduced concept implemented in the time domain with a sliding window approach [15], nonexistent in [9] [10] [12]. The key underlying idea consists in equalizing (non overlapping) groups of

symbols and then detecting their individual space-time components in a disjoint and iterative fashion. InterGroup Interference (IGI) equalization preferably relies on Minimum Mean Square Error (MMSE) criterion. Greater receiver design flexibility and potential optimization of the performance/complexity trade-off come as a result. Complementing swiftly mentioned remarks in [15], we address many algorithmic subtleties, showing how to take advantage of the new degrees of freedom at our disposal, namely the choice of the criteria retained for IGI equalization and component detection, their possible hybridization and the various scheduling options induced by the functional split (i.e., the doubly iterative structure). Particular emphasis is put on the grouping strategy which naturally emerges from the vision of MIMO communications as the transmission of multidimensional symbols on a Single-Input Multiple-Output (SIMO) channel. This shift in viewpoint was also the core of [15]. For this particular case, intergroup interference coincides with InterSymbol Interference (ISI), in multidimensional sense, while detection deals with Co-Antenna Interference (CAI) (i.e., space components). Interestingly, the conventional turbo-equalizer, inspired by Wang and Poor's seminal paper [13], where both ISI and CAI are jointly cancelled in MMSE sense [16] [17] [18], is proved to come as another particular case, in which groups are simply reduced to individual space-time components. We intentionally derive the proposed family of frequency domain block turbo-equalizers in a quite generic way in order to highlight its suitability to MIMO Multi-User (MU) and Single-User (SU) scenarios and to many space-time interleaved coding schemes, including among others Space-Time Bit-Interleaved Coded Modulation (STBICM) (see [15] and the references therein).

The paper is organized as follows. Section II introduces the communication model. Section III is the core of our contribution, in which we detail the novel turbo-equalizing concept and show how to use the Fourier domain to implement it in an efficient manner. Section IV is dedicated to numerical results, while Section V concludes the paper.

Notation

- The superscripts $^\top$ and † indicate conjugate, transpose and Hermitian transpose, respectively.
- diag$\{.\}$, tr$\{.\}$ and det$\{.\}$ denote diagonal, trace, and determinant operators on square ma-

trices, respectively.

- $\mathbb{E}\{.\}$ denotes expectation. Unless otherwise stated, bold letters $\boldsymbol{\Theta}$ and $\boldsymbol{\Xi}$ are employed for expressing covariance matrices.

- We use the proportionality symbol $\propto$ in order to indicate that the quantity in the RHS is defined up to a multiplicative factor chosen to produce a true probability mass function (pmf) or probability density function (pdf).

- Matrices are denoted by capital letters $\mathbf{M}$, with l^{th} row $\mathbf{m}^l$ and k^{th} column $\mathbf{m}_k$. Entry (l, k) is denoted $m_{l,k}$ or equivalently $[\mathbf{M}]_{l,k}$. The $L \times L$ identity matrix is denoted by $\mathbf{I}_L$ while $\mathbf{0}_L$ and $\mathbf{1}_L$ stand for the all-zero or all-one L-dimensional column vectors, respectively. From any matrix $\mathbf{M}$ of dimension $L \times N$, we can define the vector $\underline{\mathbf{m}} = vec(\mathbf{M}) = \left[\mathbf{m}_0^\intercal, \dots, \mathbf{m}_{L-1}^\intercal\right]^\intercal$ of size LN.

- $\mathbf{U}_L$ denotes the DFT unitary matrix of dimension $L \times L$ with entries $[\mathbf{U}_L]_{l,k} = \frac{1}{\sqrt{L}} e^{-j\frac{2\pi kl}{L}}$, $(l, k) \in [0, L-1]^2$.

- The block DFT matrix of dimension $LN \times LN$ is simply defined as $\mathbf{U}_{L,N} = \mathbf{U}_L \otimes \mathbf{I}_N$ where $\otimes$ is the Kronecker product.

- For any complex vector $\underline{\mathbf{x}} \in \mathbb{C}^{LN}$ made of L stacked complex subvectors of dimension N, the block DFT transform $\underline{\mathbf{x}}_f \in \mathbb{C}^{LN}$ is defined as $\underline{\mathbf{x}}_f = \mathbf{U}_{L,N}\underline{\mathbf{x}}$.

II. COMMUNICATION MODEL

We start considering a general MIMO MU scenario where N_U active users **share a pool** of N_T antennas to transmit information towards the receiver equipped with N_R antennas. The number of antenna for user u is $N_T^{(u)}$. Each user sees its own $N_R \times N_T^{(u)}$ quasi-static MIMO channel with memory M (i.e., all user channels have the same memory). The MIMO SU scenario obviously follows when all transmit antennas are given to one single user at a time. Users have no or very limited information about their channel at transmitter. Perfect channel state information is available at receiver. At the level of each user, a distinct space-time encoding Ψ_u maps a vector of information bits $\mathbf{m}_u$ of length $k_o^{(u)}$ into a codeword $\mathbf{X}_u$ which always can be put under the form of a complex matrix of dimension $N_T^{(u)} \times L$ where L stands for the space-time

code length. The set of all matrix codewords (i.e., the space-time code) for user u is denoted $\mathcal{S}_u$. The (possibly non-linear) mapping Ψ_u comprises coding (over Galois field $\mathbb{F}_2$), space-time interleaving (at bit or symbol level) and modulation (specific labeling rule per constellation per transmit dimension). We also define the overall space-time encoding Ψ which maps the vector $\mathbf{m} = [\mathbf{m}_0^\intercal \ldots, \mathbf{m}_{N_U-1}^\intercal]^\intercal$ of stacked user binary information messages (size k_o) into a codeword $\mathbf{X}$ of dimension $N_T \times L$ made of the stacked corresponding user space-time codewords, i.e.,

$$\mathbf{X} = \begin{bmatrix} \mathbf{X}_0 \\ \vdots \\ \mathbf{X}_{N_U-1} \end{bmatrix}. \tag{1}$$

Columns of $\mathbf{X}$ belong to the multidimensional constellation $\mathcal{X}$ made of the Cartesian product of all constellations $\mathcal{X}_t$, $t \in [0, N_T-1]$. Note that such a general formalism also encompasses MIMO SU with layered space-time coding architectures (e.g., [19, LST-II] [20]). Unless otherwise stated, the vision of a global space-time code $\mathcal{S} = \{\mathbf{X} = \Psi(\mathbf{m}) : \mathbf{m} \in \mathbb{F}_2^{k_o}\}$ is favored in the rest of the paper. The spectral efficiency is $\eta = k_o/L$ (in bits/c.u) under ideal Nyquist bandlimited filtering assumption. We assume $\mathbb{E}\{\mathbf{x}_k \mathbf{x}_k^\dagger\} = \mathbf{I}_{N_T}$, $\forall k$. Power distribution among users is taken into account in the additive noise covariance matrix. Moreover, considering that active users employ BICM (if they have only one transmit antenna) or STBICM (if they have multiple transmit antennas) turns out to be a good strategy to achieve spectrally-efficient power-efficient reliable communication in this particular setting. The block transmission context allows us to assume that a CP of length L_{CP} ($\geq M$) is inserted turning the complex matrix $\mathbf{X}$ into $\mathbf{X}' = \mathbf{X}\mathbf{A}_{CP}$ of dimension $N_T \times (L + L_{CP})$ where $\mathbf{A}_{CP}$ is the matrix of dimension $L \times (L + L_{CP})$ given by

$$\mathbf{A}_{CP} = \begin{bmatrix} \mathbf{0}_{(L-L_{CP})\times L_{CP}} & \mathbf{I}_{L-L_{CP}} & \mathbf{0}_{(L-L_{CP})\times L_{CP}} \\ \mathbf{I}_{L_{CP}} & \mathbf{0}_{L_{CP}\times(L-L_{CP})} & \mathbf{I}_{L_{CP}} \end{bmatrix}. \tag{2}$$

For each user, transmission occurs on $N_R \times N_T^{(u)}$ MIMO which is quasi-static, i.e., constant for $L + L_{CP}$ channel uses and fully characterized by its Finite Impulse Response (FIR) made of $M + 1$ non-zero symbol-spaced matrix taps $\mathbf{H}_0^{(u)}, ..., \mathbf{H}_M^{(u)}$ of dimension $N_R \times N_T^{(u)}$ with zero-mean circularly symmetric complex Gaussian entries satisfying the normalization mean power

constraint

$$\mathbb{E}\left[\text{diag}\left\{\sum_{m=0}^{M}\mathbf{H}_m^{(u)}\mathbf{H}_m^{(u)\dagger}\right\}\right] = N_T^{(u)}\mathbf{I}_{N_R} \ . \tag{3}$$

Free space attenuation and shadowing for each user channel are taken into account in the additive noise covariance matrix. From the user channels, we define an overall compound channel $\mathbf{H}$ made of $M + 1$ non-zero symbol-spaced matrix taps $\mathbf{H}_0, ..., \mathbf{H}_M$ of dimension $N_R \times N_T$ defined as

$$\mathbf{H}_m = \left[\begin{array}{ccc} \mathbf{H}_m^{(0)} & \dots & \mathbf{H}_m^{(N_U-1)} \end{array}\right] \ . \tag{4}$$

This again allows to treat MIMO MU and MIMO SU scenarios within a unifying formalism. Let $\mathbf{Y}'$ denote the receive matrix of dimension $N_R \times (L + L_{CP})$. After CP deletion, we obtain a new matrix $\mathbf{Y} = \mathbf{Y}'\mathbf{B}_{CP}$ of dimension $N_R \times L$ where $\mathbf{B}_{CP}$ is the matrix of dimension $(L + L_{CP}) \times L$ given by

$$\mathbf{B}_{CP} = \left[\begin{array}{c} \mathbf{0}_{L_{CP}\times L} \\ \mathbf{I}_L \end{array}\right] \tag{5}$$

whose columns $\mathbf{y}_k \in \mathbb{C}^{N_R}$, $k = 0, \dots, L - 1$, verify

$$\mathbf{y}_k = \sum_{m=0}^{M}\mathbf{H}_m\mathbf{x}_{(k-m)\,\text{mod}\,L} + \mathbf{w}_k \ . \tag{6}$$

The noise vectors $\mathbf{w}_k \in \mathbb{C}^{N_R}$ are assumed independent identically distributed (i.i.d) circularly symmetric complex with covariance matrix $\mathbf{\Theta}_{\mathbf{w}}$, i.e., the time correlation between noise vectors $\mathbf{w}_k$ is neglected. They form the matrix noise $\mathbf{W}$ of dimension $N_R \times L$. Model (6) can be rewritten in time domain under the matrix form

$$\underline{\mathbf{y}} = \mathcal{H}_c\underline{\mathbf{x}} + \underline{\mathbf{w}} \tag{7}$$

where $\underline{\mathbf{x}} = vec(\mathbf{X})$, $\underline{\mathbf{y}} = vec(\mathbf{Y})$, $\underline{\mathbf{w}} = vec(\mathbf{W})$ (covariance matrix $\mathbf{\Theta}_{\underline{\mathbf{w}}} = \mathbf{I}_L \otimes \mathbf{\Theta}_{\mathbf{w}}$) and where $\mathcal{H}_c$ is the block circulant matrix of dimension $N_R L \times N_T L$ whose first column is made of the channel impulse response appended by $(L - M - 1)$ zeros. As a result, $\underline{\mathbf{H}}_c$ can be block diagonalized in the Fourier basis, i.e., $\mathcal{H}_c = \mathbf{U}_{L,N_R}^{\dagger}\mathbf{\Lambda}\mathbf{U}_{L,N_T}$ with $\mathbf{\Lambda} = \text{diag}\{\mathbf{\Lambda}_0, \cdots, \mathbf{\Lambda}_{L-1}\}$ where

$$\mathbf{\Lambda}_l \triangleq \sum_{m=0}^{M}\mathbf{H}_m e^{-j\frac{2\pi lm}{L}} \ . \tag{8}$$

Hence, a frequency domain equivalent of (7) is

$$\underline{\mathbf{y}}_f = \mathbf{\Lambda}\underline{\mathbf{x}}_f + \underline{\mathbf{w}}_f \ . \tag{9}$$

Model (7) can also be achieved when resorting to the so called Zero Padding (ZP) with OverLap-Add (ZP-OLA) technique [22] [23] [24]. The CP is thus replaced by a ZP of identical length L_{CP} leading to the $N_T \times (L + L_{CP})$ symbol matrix $\mathbf{X}_{ZP} = \mathbf{X}\mathbf{A}_{ZP}$ with $\mathbf{A}_{ZP}$ being the $L \times (L + L_{CP})$ matrix

$$\mathbf{A}_{ZP} = \left[\begin{array}{cc} \mathbf{I}_L & \mathbf{0}_{L \times L_{CP}} \end{array} \right] = \mathbf{B}_{CP}^{\mathsf{T}} \ . \tag{10}$$

After ZP deletion, we obtain a new matrix $\mathbf{Y} = \mathbf{Y}^{'}\mathbf{B}_{ZP}$ of dimension $N_R \times L$ where $\mathbf{B}_{ZP}$ is the matrix of dimension $(L + L_{CP}) \times L$ given by

$$\mathbf{B}_{ZP} = \left[\begin{array}{cc} \mathbf{I}_{L_{CP}} & \mathbf{0}_{L_{CP} \times (L - L_{CP})} \\ \mathbf{0}_{L_{CP} \times (L - L_{CP})} & \mathbf{I}_{L - L_{CP}} \\ \mathbf{I}_{L_{CP}} & \mathbf{0}_{L_{CP} \times (L - L_{CP})} \end{array} \right] = \mathbf{A}_{CP}^{\mathsf{T}} \ . \tag{11}$$

It is evident from (10) and (11) that the ZP-OLA slightly colors the noise. However, this noise coloration can be neglected without much performance degradation. Finally, it is worth stressing that model (7) is also obtained for SCT with Interleaved Frequency-Division Multiple Access (IFDMA) [21], a promising technique for which the proposed class of block turbo-equalizers is perfectly matched.

III. A CLASS OF FREQUENCY DOMAIN BLOCK TURBO-EQUALIZERS

A. *Optimal iterative algorithm*

In order to minimize the Block Error Rate (BLER), we aim at solving the following discrete optimization problem:

$$\widehat{\mathbf{m}} = \arg \max_{\mathbf{a} \in \mathbb{F}_2^{k_o}} P\left[\mathbf{m} = \mathbf{a} \,|\, \mathbf{Y} \right] \ . \tag{12}$$

This discrete optimization problem is often reformulated as follows. Find

$$\widehat{m}_l = \arg \max_{a \in \mathbb{F}_2} \sum_{\mathbf{a} \in \mathbb{F}_2^{k_o} : a_l = a} P\left[\mathbf{X} = \Psi\left(\mathbf{a}\right) \,|\, \mathbf{Y} \right] \ . \tag{13}$$

A decision is taken on each information bit m_l based on (13) and a block error is declared whenever one estimated bit is wrong. Brute force resolution of (13) is far beyond the scope of practical feasibility. To the best of the Authors' knowledge, the most efficient method to deal with (13) consists in applying the Belief Propagation (BP) algorithm [25] [26], which iteratively approximate the pmfs corresponding to the marginals of the joint A Posteriori Probability (APP) $P\left[\mathbf{X} = \mathbf{A} \,|\, \mathbf{Y}\right]$. The BP iterative joint decoder belongs to the class of message-passing algorithms for graphical models [27]. It relies on the idea of exchanging messages, in the form of pmfs of coded symbols $\{x_{t,k}\}$, between well-chosen functional blocks. In our case, the two functional blocks are space-time detection and outer decoding (comprising symbol-to-digit soft demapping, deinterleaving and decoding in the case of STBICM). At any current iteration $i = 0, \ldots, i_{\max}$ of the algorithm, we assume available and usable the set of probabilistic messages $\mathbf{P}_{t,k}^{(i-1)} \triangleq \{P_{t,k}^{(i-1)}(a) : a \in \mathcal{X}_t\}$ where $P_{t,k}^{(i-1)}(a)$ acts as the a priori probability that the random variable $x_{t,k}$ takes realization a (delivered at iteration $i-1$). Following [15], it is understood that notation $\mathbf{P}_{t,k}^{(i-1)}$ stands for a pmf defined over the discrete alphabet $\mathcal{X}_t$. At first iteration $i = 0$, probabilistic messages $\mathbf{P}_{t,k}^{(-1)}$ are initialized with uniform pmfs.

Step 1: The space-time detection calculates the pmfs

$$Q_{t,k}^{(i)}(a) \propto \sum_{\mathbf{A} \in \mathcal{X}^L : a_{t,k} = a} p\left(\mathbf{Y} \,|\, \mathbf{A}\right) \prod_{(t',k') \neq (t,k)} P_{t',k'}^{(i-1)}(a_{t',k'}) \tag{14}$$

where

$$p\left(\mathbf{Y} \,|\, \mathbf{A}\right) \propto \exp\left\{-(\underline{\mathbf{y}} - \mathcal{H}_c\underline{\mathbf{a}})^\dagger \mathbf{\Theta}_{\underline{\mathbf{w}}}^{-1}(\underline{\mathbf{y}} - \mathcal{H}_c\underline{\mathbf{a}})\right\} . \tag{15}$$

In the turbo-decoding terminology, messages $\mathbf{Q}_{t,k}^{(i)}$'s are often referred to as EXTrinsic (EXT) pmfs on coded symbols given the observed matrix $\mathbf{Y}$ and the a priori pmfs $\mathbf{P}_{t',k'}^{(i-1)}$'s.

Step 2: The outer decoding is formally expressed as

$$P_{t,k}^{(i)}(a) \propto \sum_{\mathbf{A} = \Psi(\mathbf{m}) \in \mathcal{S} : a_{t,k} = a} \prod_{(t',k') \neq (t,k)} Q_{t',k'}^{(i)}(a_{t',k'}) . \tag{16}$$

In the turbo-decoding terminology, messages $\mathbf{P}_{t,k}^{(i)}$'s are often referred to as EXT pmfs on coded symbols given the intrinsic pmfs $\mathbf{Q}_{t',k'}^{(i)}$'s.

This completes an iteration. At each iteration, one can also compute the APPs on coded symbols defined as

$$APP_{t,k}^{(i)}(a) \propto P_{t,k}^{(i)}(a)\, Q_{t,k}^{(i)}(a) \ . \tag{17}$$

After a given number of iterations $i_{\max}$, a bit decision is made according to

$$\widehat{m}_l = \operatorname{sign} \ln \frac{\sum_{\mathbf{A}=\Psi(\mathbf{m})\in\mathcal{S}:m_l=1} \prod_{(t,k)} APP_{t,k}^{(i_{\max})}(a_{t,k})}{\sum_{\mathbf{aA}=\Psi(\mathbf{m})\in\mathcal{S}:m_l=0} \prod_{(t,k)} APP_{t,k}^{(i_{\max})}(a_{t,k})} \ . \tag{18}$$

With only two functional blocks, the scheduling is obvious. In the STBICM setting (favored in the simulation Section), pmfs $\mathbf{P}_{t,k}^{(i)}$'s are constructed from EXT pmfs (or log ratios) on coded bits fed back by the decoder (simple product assuming perfect space-time interleaving and thus symbol digit independence). Marginal EXT pmfs on symbol digits have to be extracted (by simple marginalization) from the $\mathbf{Q}_{t,k}^{(i)}$'s and serve, after space-time de-interleaving as intrinsic pmfs (or log ratios) on coded bits for the decoder.

B. New concept overview

Clearly, space-time detection is the most computationally demanding task due to the multiple sums over discrete alphabets. In order to decrease the complexity, we propose to split space-time detection into separate stages, i.e., to equalize groups of symbols in vector $\underline{\mathbf{x}}$ using the suboptimal MMSE criterion and to optimally detect symbol components within each equalized group using the MAP criterion. Let us partition the $N_T L$ symbols in $\underline{\mathbf{x}}$ into N_P groups, $\Delta_0,\ldots,\Delta_{N_P-1}$, each of them being defined as a set of index couples (t,k) with $t\in[0,N_T-1]$ and $k\in[0,L-1]$[1]. IGI appears as soon as $N_P \geq 2$. We refer the two aforementioned computation building blocks as IGI equalization and intra-group component detection. The choice of the partition should be primarily dictated by the observation of the Gram matrix $\mathcal{H}_c^\dagger \mathbf{\Theta}_{\underline{\mathbf{w}}}^{-1} \mathcal{H}_c$ (or $\mathbb{E}\left\{\mathcal{H}_c^\dagger \mathbf{\Theta}_{\underline{\mathbf{w}}}^{-1} \mathcal{H}_c\right\}$) and complexity impediments, i.e., highly correlated components should be grouped taking into account the computational feasibility of the subsequent component detection.

[1]Note that index pairs (t,k) convey the distinction between space and time dimensions (inherent to MIMO communications), which do not appear explicitly for block transmission and arbitrarily chosen partitions.

Step 1: For a specified group Δ, the IGI equalization starts computing an MMSE estimate $\mathbf{z}_{\Delta}^{(i)}$ of $\mathbf{x}_{\Delta} \triangleq [x_{t,k} : (t,k) \in \Delta]^{\mathsf{T}}$ given the observation vector $\underline{y}$ and the set of a priori pmfs $\{\mathbf{P}_{t,k}^{(i-1)} : (t,k) \notin \Delta\}$ (symbol components in Δ are premised uniformly distributed). This (biased) estimate takes the form

$$\mathbf{z}_{\Delta}^{(i)} = \mathbf{G}_{\Delta}^{(i)}\mathbf{x}_{\Delta} + \zeta_{\Delta}^{(i)} \tag{19}$$

where $\mathbf{G}_{\Delta}^{(i)}$ is a square matrix of dimension $|\Delta|$ and where $\zeta_{\Delta}^{(i)}$ is a zero-mean random vector with covariance matrix $\mathbf{\Theta}_{\zeta_{\Delta}}^{(i)}$. Using a Gaussian Approximation (GA) on the non-trivial conditional pdf $\mathbf{z}_{\Delta}^{(i)}|\mathbf{x}_{\Delta}$, the IGI equalization gives the intermediate pmfs

$$R_{\Delta}^{(i)}(\mathbf{a}) \propto \exp\left\{-(\mathbf{z}_{\Delta}^{(i)} - \mathbf{G}_{\Delta}^{(i)}\mathbf{a})^{\dagger}(\mathbf{\Theta}_{\zeta_{\Delta}}^{(i)})^{-1}(\mathbf{z}_{\Delta}^{(i)} - \mathbf{G}_{\Delta}^{(i)}\mathbf{a})\right\} \tag{20}$$

defined over the discrete alphabet $\mathcal{X}_{\Delta}$ built as the Cartesian product of the constellations involved in the definition of $\mathbf{x}_{\Delta}$.

Step 2: Component detection for group Δ computes the pmfs

$$Q_{t,k}^{(i)}(a) \propto \sum_{\mathbf{a} \in \mathcal{X}_{\Delta}:a_{t,k}=a} R_{\Delta}^{(i)}(\mathbf{a}) \prod_{(t',k') \in \Delta \setminus \{(t,k)\}} P_{t',k'}^{(i-1)}(a_{t',k'}) \ . \tag{21}$$

Step 3: Outer decoding is kept unmodified, formally expressed as

$$P_{t,k}^{(i)}(a) \propto \sum_{\mathbf{A}=\mathbf{\Psi}(\mathbf{m})\in\mathcal{S}:a_{t,k}=a} \prod_{(t',k')\neq(t,k)} Q_{t',k'}^{(i)}(a_{t',k'}) \ . \tag{22}$$

Each iteration is again concluded by the calculation of the APPs on coded symbols as

$$APP_{t,k}^{(i)}(a) \propto P_{t,k}^{(i)}(a) Q_{t,k}^{(i)}(a) \ . \tag{23}$$

and the same decision rule (18) is applied at the end. This 3-step iterative procedure gives rise to multiple scheduling options. The reference scheduling is made of one pass of each step, but nothing prevents to imagine other types of schedulings (see simulation Section).

C. Details of Wiener filters for IGI equalization

In the sequel, all conditioning are done with respect to the pmfs $\mathbf{P}_{t,k}^{(i-1)}$'s. We omit iteration index i for the sake of notation simplicity. Given the $\mathbf{P}_{t,k}$'s, we can compute the conditional vector mean $\widetilde{x}_{t,k} \triangleq \mathbb{E}\{x_{t,k}|\mathbf{P}_{t,k}\}$ and the conditional covariance $\theta_{t,k} \triangleq \mathbb{E}\{|x_{t,k} - \widetilde{x}_{t,k}|^2|\mathbf{P}_{t,k}\}$

of each coded symbol $x_{t,k}$. In compliance with model (7), let us introduce the stacked vectors $\widetilde{\underline{\mathbf{x}}} \triangleq \mathbb{E}\{\underline{\mathbf{x}} \,|\, \{\mathbf{P}_{t,k}\}\}$ and $\widetilde{\underline{\mathbf{x}}}_{|\Delta} \triangleq \mathbb{E}\{\underline{\mathbf{x}} \,|\, \{\mathbf{P}_{t,k} : (t,k) \notin \Delta\}\}$. Let $\mathbf{E}_\Delta$ be the matrix of dimension $N_T L \times |\Delta|$ defined as $\mathbf{x}_\Delta = \mathbf{E}_\Delta^\dagger \underline{\mathbf{x}}$. The achieving of the (biased) MMSE estimate (19) results from the following canonical decomposition.

Step 1: The stacked observation vector $\underline{\mathbf{y}}$ is rendered zero-mean by subtracting the mean $\widetilde{\underline{\mathbf{y}}}_{|\Delta}$ conditioned to $\{\mathbf{P}_{t,k} : (t,k) \notin \Delta\}$, expressed as

$$\widetilde{\underline{\mathbf{y}}}_{|\Delta} \triangleq \mathcal{H}_c \widetilde{\underline{\mathbf{x}}}_{|\Delta} = \mathcal{H}_c \left(\mathbf{I}_{N_T L} - \mathbf{E}_\Delta \mathbf{E}_\Delta^\dagger \right) \widetilde{\underline{\mathbf{x}}} \ . \tag{24}$$

The vector $\widetilde{\underline{\mathbf{y}}}_{|\Delta}$ models the conditional soft interference affecting group Δ.

Step 2: A biased estimate $\mathbf{z}_\Delta'$ of the vector $\mathbf{x}_\Delta$ is simply given by the output of the $|\Delta|$-dimensional Wiener filter $\mathbf{F}_\Delta'$ applied to the zero-mean observation $\underline{\mathbf{y}} - \widetilde{\underline{\mathbf{y}}}_{|\Delta}$ and minimizing the conditional Mean Square Error (MSE)

$$\mathbb{E}\left\{ \left[\mathbf{x}_\Delta - \mathbf{F}_\Delta' \left(\underline{\mathbf{y}} - \widetilde{\underline{\mathbf{y}}}_{|\Delta} \right) \right] \left[\mathbf{x}_\Delta - \mathbf{F}_\Delta' \left(\underline{\mathbf{y}} - \widetilde{\underline{\mathbf{y}}}_{|\Delta} \right) \right]^\dagger \,|\, \{\mathbf{P}_{t,k} : (t,k) \notin \Delta\} \right\} \tag{25}$$

in the sense of the stochastic matrix innerproduct $\langle \mathbf{x}, \mathbf{y} \rangle \triangleq \mathbb{E}\left\{ \mathbf{x}\mathbf{y}^\dagger \,|\, \{\mathbf{P}\} \right\}^2$. The projection theorem together with the inversion lemma yield the following expression

$$\mathbf{F}_\Delta^{'} = \mathbf{C}_\Delta^{-1} \mathbf{E}_\Delta^\dagger \mathcal{H}_c^\dagger \mathbf{A}^{-1} \tag{26}$$

in which we have introduced the following intermediate matrices

$$\begin{aligned} \mathbf{A} &= \mathcal{H}_c \boldsymbol{\Theta}_{\underline{\mathbf{x}}} \mathcal{H}_c^\dagger + \boldsymbol{\Theta}_{\underline{\mathbf{w}}} \ , \\ \mathbf{B}_\Delta &= \mathbf{E}_\Delta^\dagger \boldsymbol{\Theta}_{\underline{\mathbf{x}}} \mathbf{E}_\Delta \ , \\ \mathbf{G}_\Delta &= \mathbf{E}_\Delta^\dagger \mathcal{H}_c^\dagger \mathbf{A}^{-1} \mathcal{H}_c \mathbf{E}_\Delta \ , \\ \mathbf{C}_\Delta &= \mathbf{I}_{|\Delta|} + \mathbf{G}_\Delta \left(\mathbf{I}_{|\Delta|} - \mathbf{B}_\Delta \right) \ , \\ \boldsymbol{\Theta}_{\underline{\mathbf{x}}} &= \mathbb{E}\left\{ (\underline{\mathbf{x}} - \widetilde{\underline{\mathbf{x}}}) (\underline{\mathbf{x}} - \widetilde{\underline{\mathbf{x}}})^\dagger \,|\, \{\mathbf{P}_{t,k}\} \right\} = \mathrm{diag}\left\{ \ldots, \theta_{t,k}, \ldots \right\} \ . \end{aligned} \tag{27}$$

Indeed, assuming infinitely deep space-time interleaving, both time independence and space independence between components in vector $\underline{\mathbf{x}}$ hold and the covariance matrix $\boldsymbol{\Theta}_{\underline{\mathbf{x}}}$ is diagonal.

---

[2]Note that such a MSE implies the minimization of the MSE associated with the conventional stochastic innerproduct $\langle \mathbf{x}, \mathbf{y} \rangle \triangleq \mathbb{E}\left\{ \mathbf{x}^\dagger \mathbf{y} \,|\, \{P(\cdot)\} \right\} = \mathbb{E}\left\{ \mathrm{tr}\left\{ \mathbf{x}\mathbf{y}^\dagger \,|\, \{P(\cdot)\} \right\} \right\}$.

The output of the Wiener filter $\mathbf{F}_{\Delta}^{'}$ is given by

$$\mathbf{z}_{\Delta}^{'} = \mathbf{F}_{\Delta}^{'}\left(\underline{\mathbf{y}} - \widetilde{\underline{\mathbf{y}}}_{|\Delta}\right) = \mathbf{C}_{\Delta}^{-1}\mathbf{G}_{\Delta}\mathbf{x}_{\Delta} + \zeta_{\Delta}^{'} \ . \tag{28}$$

Step 3: Since the Signal-to-interference plus Noise Ratio (SINR) per component at the output of the IGI equalizer is invariant by left multiplication by any square constant invertible matrix of dimension $|\Delta|$, we can rather consider the output

$$\mathbf{z}_{\Delta} = \mathbf{C}_{\Delta}\mathbf{z}_{\Delta}^{'} = \mathbf{G}_{\Delta}\mathbf{x}_{\Delta} + \zeta_{\Delta} \tag{29}$$

of the filter $\mathbf{F}_{\Delta} = \mathbf{C}_{\Delta}\mathbf{F}_{\Delta}^{'} = \mathbf{E}_{\Delta}^{\dagger}\mathcal{H}_{c}^{\dagger}\mathbf{A}^{-1}$. In (29), $\zeta_{\Delta} \in \mathbb{C}^{|\Delta|}$ is a zero-mean random vector of residual (ISI+thermal) noise with conditional covariance matrix

$$\boldsymbol{\Theta}_{\zeta_{\Delta}} = \mathbb{E}\left\{\zeta_{\Delta}\zeta_{\Delta}^{\dagger} \,|\, \{\mathbf{P}_{t,k} : (t,k) \notin \Delta\}\right\} = \mathbf{G}_{\Delta}\left(\mathbf{I}_{|\Delta|} - \mathbf{B}_{\Delta}\mathbf{G}_{\Delta}\right) \ . \tag{30}$$

As already pointed out in few contributions, computing decision statistics $\widetilde{x}_{t,k}$ and $\theta_{t,k}$ with $\mathbf{APP}_{t,k}$'s instead of EXT pmfs $\mathbf{P}_{t,k}$'s introduces a conditional negative bias in the vector residual (ISI+thermal) noise vector ζ_{Δ} which tends to cancel the useful signal component in model (19). In order to fight back this detrimental effect, some authors (see, for example, [28] [29] in the context of multiuser turbo-detection for CDMA) have tried to justify the calculation of decision statistics with EXT pmfs by invoking the basic rules governing the BP algorithm [25]. However, we empirically witnessed that better performance (i.e., better conditional interference estimation) is sometimes achieved when all the information sources at disposal (i.e., including channel observation) are used and that mitigation of the bias effect appears after few iterations (no oscillatory behavior, faster convergence). We will not elaborate on this quite intricate rather difficult to analyze subject, having no satisfactory theoretic explanation yet.

The complexity of the IGI equalization step is largely dominated by the inversion of the square matrix $\mathbf{A}$ of dimension $N_R L$ (done only once for all groups). We note that, due to the conditional covariance matrix $\boldsymbol{\Theta}_{\underline{\mathbf{x}}}$, matrix $\mathbf{A}$ is not block circulant despite the CP operations. Besides, the calculation of pmfs (20) for the particular group Δ obviously requires the inversion of (30) of dimension $|\Delta|$. This additional complexity may not be negligible for large groups.

D. Efficient frequency domain implementation

For efficient computation of $\mathbf{A}^{-1}$ in the Fourier domain, the unconditional approximation is the key, that basically consists in minimizing the ensemble (or block) Mean Square Error (MSE) instead of the conditional instantaneous MSE (25) [30]. Doing so, the conditional variances $\theta_{t,k}$ are replaced by their ensemble average as

$$\xi_t = \mathbb{E}\left\{\theta_{t,k}\right\} \tag{31}$$

which, in practice, are evaluated using the consistent estimator

$$\xi_t \simeq \frac{1}{L}\sum_{k=0}^{L-1} \theta_{t,k} \ . \tag{32}$$

The conditional covariance matrix $\boldsymbol{\Theta}_{\underline{\mathbf{x}}}$ is replaced by its ensemble average as

$$\boldsymbol{\Xi}_{\underline{\mathbf{x}}} = \mathbb{E}\left\{\boldsymbol{\Theta}_{\underline{\mathbf{x}}}\right\} = \mathbf{I}_L \otimes \boldsymbol{\Xi} \tag{33}$$

with

$$\boldsymbol{\Xi} = \mathrm{diag}\left\{\xi_0, \ldots, \xi_{N_T-1}\right\} \ . \tag{34}$$

When substituting (33) for $\boldsymbol{\Theta}_{\underline{\mathbf{x}}}$ in matrix $\mathbf{A}$, the latter becomes block circulant and can be block diagonalized in the Fourier basis as

$$\mathbf{A} = \mathbf{U}_{L,N_R}^{\dagger} \left(\boldsymbol{\Lambda}\boldsymbol{\Xi}_{\underline{\mathbf{x}}}\boldsymbol{\Lambda}^{\dagger} + \boldsymbol{\Theta}_{\underline{\mathbf{w}}}\right) \mathbf{U}_{L,N_R} \ . \tag{35}$$

From (35), we deduct that the computation of $\mathbf{A}^{-1}$ in the Fourier domain requires the inversions of L square matrices of (much reduced) dimension N_R. The complexity is linear in the space-time code length L and cubic in the number of receive antennas N_R. In contrast with the time domain sliding-window approach [15], it is insensitive to the channel memory M, which constitutes an obvious advantage for very high-data rate MIMO systems (large ISI span).

The second aforementioned complexity impediment concerns the inversion of covariance matrices (30) for the different groups. We first note that the matrix $\mathcal{H}_c^{\dagger}\mathbf{A}^{-1}\mathcal{H}_c$, involved in the calculation of $\mathbf{G}_{\Delta}$ is block circulant and can be block diagonalized in the Fourier basis as

$$\mathcal{H}_c^{\dagger}\mathbf{A}^{-1}\mathcal{H}_c = \mathbf{U}_{L,N_T}^{\dagger}\boldsymbol{\Lambda}^{\dagger}\left(\boldsymbol{\Lambda}\boldsymbol{\Xi}_{\underline{\mathbf{x}}}\boldsymbol{\Lambda}^{\dagger} + \boldsymbol{\Theta}_{\underline{\mathbf{w}}}\right)^{-1}\boldsymbol{\Lambda}\mathbf{U}_{L,N_T} \ . \tag{36}$$

It is clear that arbitrarily chosen partitions yield Δ-dependent expressions of matrices $\mathbf{B}_\Delta$ and $\mathbf{G}_\Delta$. Conversely, we are interested by well-structured partitions having the nice property to render $\mathbf{B}_\Delta$ and $\mathbf{G}_\Delta$ Δ-independent, so that only one inversion of (30) is required. Partitions of such type involve groups of equal cardinality made of consecutive constellation symbols. They are compactly described as: $N_P = L/N_s$ (with $N_s \in \mathbb{N}^*$ dividing L) and

$$\Delta_n = \{(0, nN_s), \ldots, (N_T - 1, nN_s), \ldots$$
$$\ldots, (0, (n+1)N_s - 1), \ldots, (N_T - 1, (n+1)N_s - 1)\}, \ \forall n \in [0, N_P - 1] \ . \tag{37}$$

For these partitions, matrices $\mathbf{B}_{\Delta_n}$ and $\mathbf{G}_{\Delta_n}$ have identical expressions given by

$$\mathbf{E} = \begin{bmatrix} \mathbf{I}_{N_s N_T} & \mathbf{0}_{N_s N_T \times N_s N_T (L_s - 1)} \end{bmatrix}^\top \ ,$$
$$\mathbf{B} = \mathbf{E}^\dagger \mathbf{\Xi}_{\underline{\mathbf{x}}} \mathbf{E} = \mathbf{I}_{N_s} \otimes \mathbf{\Xi} \ ,$$
$$\mathbf{G} = \mathbf{E}^\dagger \mathbf{U}_{L, N_T}^\dagger \mathbf{\Lambda}^\dagger \left(\mathbf{\Lambda} \mathbf{\Xi}_{\underline{\mathbf{x}}} \mathbf{\Lambda}^\dagger + \mathbf{\Theta}_{\underline{\mathbf{w}}} \right)^{-1} \mathbf{\Lambda} \mathbf{U}_{L, N_T} \mathbf{E} \ .$$

Great attention is given to the subcase $N_s = 1$. Indeed, for this natural partition, groups $\{\Delta_n\}$ defined as

$$\Delta_n = \{(0, n), \ldots, (N_T - 1, n)\}, \ \forall n \in [0, L - 1] \tag{38}$$

simply refer to columns of $\mathbf{X}$, i.e., to vector constellation symbols and IGI coincides with ISI (in N_T-dimensional sense). Nothing prevents using the (natural) time index k (instead of n) to identify the groups. Matrices $\mathbf{B}_{\Delta_k}$ and $\mathbf{G}_{\Delta_k}$ have identical expressions given by

$$\mathbf{B} = \mathbf{\Xi} \ ,$$
$$\mathbf{G} = \frac{1}{L} \sum_{l=0}^{L-1} \mathbf{\Lambda}_l^\dagger \left(\mathbf{\Lambda}_l \mathbf{\Xi} \mathbf{\Lambda}_l^\dagger + \mathbf{\Theta}_{\mathbf{w}} \right)^{-1} \mathbf{\Lambda}_l \ . \tag{39}$$

In compliance with (7) (9), the ISI equalization part of the turbo-equalizer is summed up in the following set of equations

$$\underline{\mathbf{z}}_f = \mathbf{\Phi} \underline{\mathbf{y}}_f - \mathbf{\Psi} \underline{\widetilde{\mathbf{x}}}_f \ ,$$
$$\mathbf{\Phi} = \mathbf{\Lambda}^\dagger \left(\mathbf{\Lambda} \mathbf{\Xi}_{\underline{\mathbf{x}}} \mathbf{\Lambda}^\dagger + \mathbf{\Theta}_{\underline{\mathbf{w}}} \right)^{-1} \ , \tag{40}$$
$$\mathbf{\Psi} = \mathbf{\Lambda}^\dagger \left(\mathbf{\Lambda} \mathbf{\Xi}_{\underline{\mathbf{x}}} \mathbf{\Lambda}^\dagger + \mathbf{\Theta}_{\underline{\mathbf{w}}} \right)^{-1} \mathbf{\Lambda} - \mathbf{I}_L \otimes \mathbf{G} \ .$$

The MMSE estimate $\mathbf{z}_k$ of constellation symbol $\mathbf{x}_k$ is simply extracted from $\underline{\mathbf{z}}_f$ as $\mathbf{z}_k = \mathbf{E}_k^\dagger \mathbf{U}_{L, N_T}^\dagger \underline{\mathbf{z}}_f$.

We also detail a third partition, which does not possess the desired property, but for which the computational complexity is minimized. It is compactly described as: $N_P = N_T L$ and $\forall n \in [0, N_P - 1]$ such that $n = kN_T + t$ with $t \in [0, N_T - 1]$, $k \in [0, L - 1]$

$$\Delta_n = \{(t, k)\} \ . \tag{41}$$

Each group Δ_n refers to a single constellation symbol $x_{t,k}$. For this conventional partition, the matrices $\mathbf{B}_{\Delta_n}$ and $\mathbf{G}_{\Delta_n}$ are reduced to scalars denoted $b_{t,k}$ and $g_{t,k}$. Taking into account the cyclic structure of $\boldsymbol{\Xi}_{\underline{\mathbf{x}}}$, there are only N_T such scalars to compute. More precisely, expressions of $b_{t,k}$ and $g_{t,k}$ are k-independent and given by

$$
\begin{aligned}
\mathbf{e}_t &= [\mathbf{0}_t^{\mathsf{T}} \ 1 \ \mathbf{0}_{N_T - t - 1}^{\mathsf{T}}]^{\top} \ , \\
b_{t,k} &= b_t = \mathbf{e}_t^{\dagger} \boldsymbol{\Xi} \mathbf{e}_t = \xi_t, \ \forall k \ , \\
g_{t,k} &= g_t = \mathbf{e}_t^{\dagger} \left[\tfrac{1}{L} \sum_{l=0}^{L-1} \boldsymbol{\Lambda}_l^{\dagger} \left(\boldsymbol{\Lambda}_l \boldsymbol{\Xi} \boldsymbol{\Lambda}_l^{\dagger} + \boldsymbol{\Theta}_{\mathbf{w}} \right)^{-1} \boldsymbol{\Lambda}_l \right] \mathbf{e}_t, \ \forall k \ .
\end{aligned}
\tag{42}
$$

In fact, this partition yields the conventional Wang and Poor's algorithm [13] (derived in the context of MIMO transmissions [16] [17] and revisited with the unconditional approximation [18]), for which ISI and CAI are jointly cancelled in MMSE sense. The set of equations (40) still sums up the MMSE ISI equalization and MMSE-based CAI cancellation parts of the turbo-equalizer with $\mathbf{G} = \mathrm{diag}\{g_0, \ldots, g_{N_T-1}\}$ in $\boldsymbol{\Psi}$. The MMSE estimate $z_{t,k}$ of constellation symbol $x_{t,k}$ is similarly extracted from $\underline{\mathbf{z}}_f$ as $z_{t,k} = \mathbf{e}_{t,k}^{\dagger} \mathbf{U}_{L,N_T}^{\dagger} \underline{\mathbf{z}}_f$ where $\mathbf{e}_{t,k} = [\mathbf{0}_{kN_T+t}^{\mathsf{T}} \ 1 \ \mathbf{0}_{LN_T - t - kN_T - 1}^{\mathsf{T}}]^{\top}$. Our novel concept thus establishes a smooth transition from the optimal BP algorithm (for which there exists a single group, the entire block, and no IGI) to the well-known Wang and Poor's algorithm (for which groups are restricted to a single space-time component).

E. Criteria hybridization

The idea of replacing the Wiener filters $\mathbf{F}_{\Delta}$ by simple Matched-Filters (MFs) $\mathbf{F}_{\Delta}^{MF} = \mathbf{E}_{\Delta}^{\dagger} \mathcal{H}_c^{\dagger}$ during the course of iterations was originally addressed in [7] [31] for time-invariant single-antenna ISI channels and later generalized to MIMO fading channels in [32] [33]. The expression of the covariance matrix (30) is modified as

$$
\boldsymbol{\Theta}_{\zeta_{\Delta}} = \mathbf{E}_{\Delta}^{\dagger} \mathcal{H}_c^{\dagger} \mathcal{H}_c \left(\boldsymbol{\Theta}_{\underline{\mathbf{x}}} - \mathbf{E}_{\Delta} \boldsymbol{\Theta}_{\underline{\mathbf{x}}} \mathbf{E}_{\Delta}^{\dagger} \right) \mathcal{H}_c^{\dagger} \mathcal{H}_c \mathbf{E}_{\Delta} + \mathbf{E}_{\Delta}^{\dagger} \mathcal{H}_c^{\dagger} \boldsymbol{\Theta}_{\underline{\mathbf{w}}} \mathcal{H}_c \mathbf{E}_{\Delta} \ . \tag{43}
$$

In [31], an EXIT chart analysis is conducted to properly characterize the convergence behavior of those hybrid iterative procedures. Such an analysis cannot be trivially enlarged to the case of non-ergodic MIMO channels. Fortunately, the observed phenomena do not depend on the particular transmission scenario and provide us design guidelines. Clearly, MF-based IGI equalization fails in early iterations when the load per antenna becomes too important (superior to 1 bit/c.u/antenna) [34] but works well once the quality of the regenerated soft interference is "good enough". To achieve this goal, we suggest the threefold strategy: first, always start with MMSE IGI equalization; second, employ $\mathbf{APP}_{t,k}$'s instead of EXT pmfs $\mathbf{P}_{t,k}$'s to compute the conditional decision statistics $\{\widetilde{x}_{t,k}\}$ and $\{\theta_{t,k}\}$; third, introduce a modified scheduling in which several inner iterations are performed between intra-group component detection and outer decoding before reactivating IGI equalization. With such a modified scheduling, the receiver can be viewed as a doubly iterative structure (i.e., made of multiple embedded iterative loops).

When the cardinality of the groups is high, the exact calculation of probabilistic messages $\mathbf{Q}_{t,k}$'s may become computationally heavy, entailing the resort to sub-optimal reduced-complexity algorithms. Prominent among them is the List-APP Sphere Decoder (LSD) [37], whose complexity is less sensitive to the alphabet size $\mathcal{X}_{\Delta}$. Another reduced-complexity option would consist in switching on MMSE-based intra-group interference cancellation [29]. On this subject, it is worth reminding that, whatever be the chosen partition, MMSE IGI equalization followed by MMSE-based intra-group interference cancellation yields nothing but the turbo-equalizer defined with the conventional partition as long as a reference scheduling is applied [15, Appendix]. This result is no longer valid with a modified scheduling, however.

Finally, an oversimplified class of turbo-equalizers can be obtained by combining the two aforementioned ideas, i.e., MF-based IGI equalization (after convergence) and MMSE-based intra-group interference cancellation. Such very-low complexity turbo-equalizers provide good performance for large MIMO systems and weak loads (typically up to 1 bit/c.u/antenna).

IV. NUMERICAL RESULTS AND DISCUSSION

A. Simulation setting

In this paper, we restrict ourselves to SU MIMO communication scenarios and put emphasis on the performance of the turbo-equalizer derived with the natural partition and different scheduling/hybridization options[3]. The single user employs a STBICM with the following characteristics: rate-$3/4$ 64-state non-recursive convolutional code with $d_{free} = 6$, 16-QAM modulation (Gray labeling). The block length is $L = 192$ ($k_o = 2304$ bits included tail). The cyclic prefix length is equal to the channel memory ($L_{CP} = M$). Transmission occurs on quasi-static 2×2 or 4×4 MIMO channels with $M = 2$ and EXPonential decreasing taps (EXP3): on each link (r, t), the $M + 1$ channel coefficients are i.i.d circularly symmetric complex Gaussian following pdfs $\mathcal{CN}(0, \sigma_m^2)$ with $\sigma_m^2 \propto \exp(-2m)$, $\forall m$. The spectral efficiency is $\eta = 6$ bits/c.u. and $\eta = 12$ bits/c.u, respectively. The noise vectors $\mathbf{w}_k$ are assumed circularly symmetric complex Gaussian and spatially uncorrelated, i.e., $\mathbf{\Theta_w} = \sigma^2 \mathbf{I}_{N_R}$. Space component detection always relies on MAP criterion. For the 4×4 MIMO channel, the optimal MAP detector is far too complex. It is practically implemented using the LSD described in [37]. The spherical list is centered on the Maximum Likelihood (ML) point instead of the received point. The ML point is computed thanks to an accelerated LSD based on the Schnorr-Euchner enumeration strategy. If not otherwise stated, the LSD origin centered list size is fixed to 10000 points. Particular attention is given to the region of BLock Error Rate (BLER) above 10^{-2} as a retransmission protocol is in place [35]. The outage probability is always given as a reference curve [36]. One iteration of the reference scheduling comprises one pass of ISI equalization, space component detection and outer decoding. Unless otherwise stated, 5 iterations are necessary to converge. In this section, we compare:

1) The turbo-equalizer derived in [18] and corresponding to conventional partition, MMSE

---

[3]As expected, we witnessed that the frequency domain block turbo-equalizers provide slightly better performance than their time domain counterparts with a sliding-window approach [15], while keeping a complexity independent of the channel memory M. Consequently, simulation results and comments in [15, Section V] keep all their relevance here, demonstrating the interest of the natural partition over the conventional one.

ISI equalization, MMSE-based CAI cancellation and reference scheduling (referred to as *Conv. MMSE* in the figure legends).

2) The turbo-equalizer derived with natural partition, MMSE ISI equalization, MAP space component detection, and reference scheduling (referred to as *Nat. MAP* in the figure legends).

3) The same with SubMAP space component detection (LSD) (referred to as *Nat. LSD* in the figure legends).

4) The turbo-equalizer derived with natural partition, MMSE ISI equalization, MAP space component detection and modified scheduling (referred to as *Nat. Doubly MAP* in the figure legends). The modified scheduling performs 3 inner iterations between space component detection and outer decoding during the first two iterations. We witness that only 3 iterations are necessary to converge.

5) The same with SubMAP space component detection (LSD) (referred to as *Nat. Doubly LSD* in the figure legends).

6) The turbo-equalizer derived with natural partition, MMSE ISI equalization at first iteration and MF ISI equalization for the subsequent iterations, SubMAP space component detection (LSD) and reference scheduling (referred to as *Nat. Hybrid LSD* in the figure legends).

7) The turbo-equalizer derived with natural partition, MMSE ISI equalization at first iteration and MF ISI equalization for the subsequent iterations, SubMAP space component detection (LSD) and modified scheduling (referred to as *Nat. Hybrid Doubly LSD* in the figure legends). The modified scheduling performs 5 inner iterations between space component detection and outer decoding at first iteration.

B. Turbo-equalization with reference scheduling

In Fig. 1, we address the impact of the prefix operations performed at the transmitter side considering the *Nat. MAP* turbo-equalizer. A slight performance loss is caused by the noise coloration induced by the ZP-OLA technique. This degradation is mainly visible at low SNRs. In Fig. 2 the improvement brought by APP-based over EXT-based interference regeneration/subtraction

is shown for *Nat. MAP* and *Conv. MMSE* turbo-equalizers. It is more pronounced for the *Conv. MMSE* turbo-equalizer (3 dB at BLER 10^{-2}). However, a 3 dB gap remains at BLER 10^{-3} between the two turbo-equalizers, proving the interest of the natural partition. In the sequel, we only consider APP-based interference regeneration/subtraction and CP insertion.

C. Turbo-equalization with modified scheduling

This subsection deals with the impact of the scheduling. In Fig. 3, we consider a 2×2 quasi-static channel. Fig. 4 envisages a quasi-static 4×4 MIMO channel, which necessitates the use of the LSD. Interestingly, we witnessed that for the *Nat. Doubly LSD* turbo-equalizer, the origin-centered list could be reduced to 5000 points without significant performance degradation. The average number of candidates N_{cand} per block and per iteration used to evaluate the $\mathbf{Q}_{t,k}$'s (with respect to some SNR values) is reported in Table I for both *Nat. LSD* and *Nat. Doubly LSD* turbo-equalizers.

E_b/N_0 (dB)	0	2	4	5	6	7
N_{cand} (*Nat. LSD*)	1419	1526	1542	1545	1549	1553
N_{cand} (*Nat. Doubly LSD*)	882	904	924	945	953	963

Table I. Average number of candidates for LSD

By reference, exhaustive MAP space detection would require the computation of $2^{16} = 65536$ likelihoods. In Fig. 3 and 4, we observe that BLER performance are similar for the *Nat.* and *Nat. Doubly* turbo-equalizer types. The gap to the outage probability is (only) 4 dB for the 2×2 channel and 3.5 dB for the 4×4 channel at BLER 10^{-2}. Taking into account the respective LSD number of candidates, we conclude that modifying the scheduling allows to save complexity.

D. Impact of antenna correlation

Finally, we investigate the ability of different types of turbo-equalizers to fight back spatial antenna correlation. The correlated MIMO channel taps $\mathbf{H}_m$'s can be expressed as

$$\mathbf{H}_m = \mathbf{R}_{N_R}^{1/2} \, \mathbf{H}_m^w \, \mathbf{R}_{N_T}^{1/2}, \ \forall m \tag{44}$$

where the $\mathbf{H}_m^w$'s stands for the uncorrelated taps and where $\mathbf{R}_{N_T}$ and $\mathbf{R}_{N_R}$ stand for the N_T dimensional transmit covariance matrix and the N_R dimensional receive covariance matrix, respectively. This model occurs when all transmit and receive antennas are closely located and have identical radiation pattern. Following [38], we take

$$\mathbf{R}_{N_T} = \mathbf{R}_{N_R} = \begin{bmatrix} 1 & \delta & \delta & \delta \\ \delta & 1 & \delta & \delta \\ \delta & \delta & 1 & \delta \\ \delta & \delta & \delta & 1 \end{bmatrix} \tag{45}$$

where $0 \leq \delta \leq 1$. It assumes that the correlation is identical between all transmit and receive antennas. This obviously represents a worst case for we can reasonably expect that the antenna correlation decreases with the distance. We consider anew the transmission over a 4×4 EXP3 MIMO channel. In Fig. 5, the performance of the *Nat. LSD* turbo-equalizer is plotted and compared to the performance offered by the *Conv. MMSE* turbo-equalizer for a correlation factor $\delta = 0.6$. Clearly, the latter is not able to deal with such a scenario. It performs 8.5 dB from the outage probability curve at BLER 10^{-2}. The gain brought by the *Nat. LSD* turbo-equalizer is almost 4 dB at BLER 10^{-2}. The performance of the *Nat. LSD* turbo-equalizer for both spatially correlated and uncorrelated MIMO channels is then addressed in Fig. 6. For a fixed outage probability of 10^{-2}, the correlated channel capacity loss amounts to 3.5 dB for $\delta = 0.6$ and 6.4 dB for $\delta = 0.8$. However, the turbo-equalizer performance degradation is worse amounting to 4.5 dB for $\delta = 0.6$ and 9 dB for $\delta = 0.8$. These results confirm that even this powerful turbo-equalizer faces some difficulties to treat severe antenna correlation. Nonetheless, it is much more efficient for this task than the *Conv. MMSE* turbo-equalizer. In Fig. 7, *Conv. MMSE*, *Nat. LSD*, *Nat. Hybrid LSD* and *Nat. Hybrid Doubly LSD* turbo-equalizers are compared again for a 4×4 EXP3 MIMO channel and a correlation factor $\delta = 0.6$. The *Nat. Hybrid Doubly LSD* turbo-equalizer performs only 1 dB away from the *Nat. LSD* turbo-equalizer at BLER 10^{-2}. Furthermore, it allows 1.5 dB gain compared to the *Nat. Hybrid LSD* one. Note that the *Nat. Hybrid Doubly LSD* turbo-equalizer also employs an origin centered list

of 5000 points. To conclude, the *Nat. Hybrid Doubly LSD* turbo-equalizer offers an excellent performance complexity trade-off in this particular transmission scenario.

V. CONCLUSION

This paper has presented a new class of block turbo-equalizers for single-carrier space-time coded transmission over MIMO broadband wireless channel. The key underlying idea consists in equalizing groups of transmitted symbols and then detecting their individual space-time components in a disjoint and iterative fashion. This functional split naturally induces new design degrees of freedom that have been accurately listed and described, i.e., choice of distinct criteria for IGI equalization and intra-group component detection, yielding hybrid structures, multiple iterative loops and related scheduling variants. Hence, our novel concept comes in a variety of algorithms that have been compared in terms of performance under various transmission scenarios. For all of them, MMSE equalization certainly occupies a central role (at least for the first iteration) and may be identified as the computational bottleneck. Fortunately, block spread transmission together with cyclic prefix operations make the channel matrix block circulant, thus allowing low complexity inversion in the Fourier domain (under mild conditions carefully specified in the paper). We believe that a full comprehension of the fine dynamics governing the overall iterative process is now necessary to better optimize the performance/complexity trade-off for a specific transmission scenario. This almost surely goes through the definition of relevant analyzing tools. Density evolution or information geometry constitute promising research avenues in this prospect. The behaviour of this class of turbo-equalizers in the presence of intra and intercell interferences is also an interesting future research topic, notably the impact of neglecting the interference time correlation necessary for their efficient frequency domain implementations.

REFERENCES

[1] Z.Wang, G.B. Giannakis, "Wireless Multicarrier Communications (where Fourier meets Shannon)," *IEEE Signal Processing Mag.*, vol. 17, no. 3, pp. 29-48, May 2000.

[2] D. Falconer, S. Kaiser, "Broadband Frequency Domain-Based Air Interferences for Future-Generation Wireless Systems," *WWRF13*, WG4, Jeju, South Korea, March 2005. Available at *http://wg4.ww-rf.org/GFD6.pdf.*

[3] H. Sari, G. Karam, I. Jeanclaude, "frequency domain Equalization of Mobile Radio and Terrestrial Broadcast Channels," *IEEE GLOBECOM'94,* San Fransisco, CA, USA, Nov.-Dec. 1994.

[4] H. Sari, G. Karam, I. Jeanclaude, "Transmission Techniques for Digital Terrestrial TV Broadcasting," *IEEE Commun. Mag.*, pp.100-109, Feb. 1995.

[5] D.Galda, H. Rohling, "A Low Complexity Transmitter Structure for OFDM-FDMA Uplink Systems," *IEEE VTCS'02*, Birmingham, Alabama, May 2002.

[6] G.K. Kaleh, "Channel Equalization for block transmission systems," *IEEE J. Sel. Areas Commun.*, vol. 13, no. 1, pp. 110-121, Jan. 1995.

[7] M. Tüchler, J. Hagenauer, "Turbo Equalization using Frequency Domain Equalizers," *Allerton Conference*, Monticello, IL, USA, Oct 2000.

[8] N. Benvenuto, S. Tomasin, "Block Iterative DFE for Single Carrier Modulation," *IEE Electronics Letters*, vol. 38, no. 19, pp. 1144-1145, Sept. 2002.

[9] D. Falconer, S.L. Ariyavisitakul, A. Benyamin-Seeyar, B. Eidson, "Frequency Domain Equalization for Single-Carrier Broadband Wireless Access Systems," *IEEE Commun. Mag.*, vol. 40, no. 4, pp. 58-66, Apr. 2002.

[10] R. Dinis, R. Kalbazi, D. Falconer, A.H. Banihashemi, "Iterative Layered Space-Time Receivers for Single-Carrier Transmission over Severe Time-Dispersive Channels," *IEEE Commun. Letters*, vol. 8, no. 9, pp. 579-581, Sept. 2004.

[11] R. Kalbasi, R. Dinis, D. Falconer, A.H. Banihashemi, "Hybrid Time-Frequency Layered Space-Time Receivers for Severe Time-Dispersive Channels," *SPAWC'04*, 2004.

[12] Fabrizio Pancaldi, G.M. Vitteta, "Block Channel Equalization in the Frequency Domain," *IEEE Trans. Commun.*, vol. COM-53, no. 3, Mar. 2005.

[13] X. Wang, H.V. Poor, "Iterative (Turbo) Soft-Interference Cancellation and Decoding for Coded CDMA," *IEEE Trans. Commun.*, vol. COM-47, no. 7, pp. 1046-1061, July 1999.

[14] M. Tüchler, R. Koetter, A. Singer, "Turbo Equalization: Principles and New Results," *IEEE Trans. Commun.*, vol. COM-50, no. 5, pp. 754-767, May 2002.

[15] R. Visoz, A.O. Berthet, S. Chtourou, "A New Class of Iterative Equalizers for Space-Time BICM over MIMO Block Fading ISI AWGN Channel," *IEEE Trans. Commun.,* vol. COM-53, no. 12, pp. 2076-2091, Dec. 2005.

[16] H. El Gamal, R. Hammons, "A New Approach to Layered Space-Time Coding and Signal Processing," *IEEE Trans. Inform. Theory*, vol. IT-47, no. 6, pp. 2321-2334, Sept. 2001.

[17] T. Abe, T. Matsumoto, "Space-Time Turbo Equalization in Frequency-Selective MIMO Channels," *IEEE Trans. Veh. Tech.*, vol. VEH-52, no. 3, pp. 469-475, May 2003.

[18] X. Wautelet, A. Dejonghe, L. Vandendorpe, "MMSE-based fractional turbo receiver for space-time BICM over frequency-selective MIMO fading channels," *IEEE Trans. Signal Processing*, Vol. SIG-52, pp. 1804-1809, June 2004.

[19] S. Ariyavisitakul, "Turbo Space-Time Processing to Improve Wireless Channel Capacity," *IEEE Trans. Commun.*, vol. COM-48, no. 8, pp. 1347-1358, Aug. 2000.

[20] N. Veselinovic, T. Matsumoto, "Reduced Complexity MIMO Turbo Equalization for STTRC-Codes," IEEE PIMRC'04, Barcelona, Spain, pp. 269-273, Sept. 2004.

[21] U. Sorger, I. De Broeck and M. Schnell, "Interleaved FDMA - A New Spread-Spectrum Multiple-Access Scheme," *IEEE ICC'98*, Atlanta, USA, June 1998.

[22] G.B. Giannakis, "Filterbanks for Blind Channel Identification and Equalization," *IEEE Sig. Proc. Lett.,* vol.4, pp.184-187, Jun. 1997.

[23] R. Crochiere, L. Rabine, "Multirate Digital Signal Processing," Englewood Cliffs, NJ: Prentice-Hall, 1983.

[24] B. Muquet, Z. Wang, G. Giannakis, M. de Courville, P. Duhamel, "Cyclic Prefixing or Zero Padding for Wireless Multicarrier Transmissions?," *IEEE Trans. Commun.,* vol. 50, no. 12, Dec. 2002.

[25] F. Kschischang, B. Frey, A. Loeliger, "Factor Graphs and the Sum-Product Algorithm," *IEEE Trans. Inform. Theory*, vol. IT-47, no. 2, pp. 498-519, Feb. 2001.

[26] T. Richardson, R. Urbanke, "The Capacity of Low-Density Parity Check Codes under Message Passing Decoding," *IEEE Trans. Inform. Theory*, vol. IT-47, no. 2, pp. 599-618, Feb. 2001.

[27] J. Pearl, "Probabilistic Reasoning in Intelligent Systems: Networks of Plausible Inference," Morgan Kaufmann, San Fransisco, 1988.

[28] S. Marinkovic, B. Vucetic, J. Evans, "Improved Iterative Interference Cancellation," *IEEE ISIT'01*, Geneva, Switzerland, May 2001.

[29] J.J. Boutros, G. Caire, "Iterative Multiuser Decoding: Unified Framework and Asymptotic Performance Analysis," *IEEE Trans. Inform. Theory*, vol. IT-48, no. 7, pp. 1772-1793, July 2002.

[30] G. Caire, R. Müller, "The Optimal Received Power Distribution of IC-based Iterative Multiuser Joint Decoders," 39th *Annual Allerton Conf. on Commun., Cont. and Comp.*, Monticello, Illinois, USA, Oct. 2001.

[31] M. Tüchler, R. Koetter, A. Singer, "Hybrid Equalization Strategies for Iterative Equalization and Decoding," *ISIT'01*, Washington, DC, USA, p. 267, 2001.

[32] H. Omori, T. Asai, T. Matsumoto, "A Matched Filter Approximation for SC/MMSE Iterative Equalizer," *IEEE Commun. Lett.*, vol.5, no. 7, pp. 310-312, July 2001.

[33] K. Kansanen, T. Matsumoto, "A Computationally Efficient MIMO Turbo-Equalizer," *IEEE VTCS'03*, Seoul, Korea, pp. 277-281, Apr. 2003.

[34] R. Visoz, S. Chtourou, A.O. Berthet " Space-Time Turbo Equalization: Performance and Complexity Trade-Off" IEEE ISCCSP06, Marrakech, Morocco, March 2006.

[35] D. Tunitelli, G. Caire, "The Throughput of Hyvrid-ARQ Protocols for the Gaussian Collision Channel," *IEEE Trans. Inform. Theory*, vol. IT-5, no. 2, pp. 1971-1988, July 2001.

[36] E. Malkamäki, H. Leib, "Coded Diversity on Block-Fading Channel," *IEEE Trans. Inform. Theory*, vol. IT-45, no. 2, pp. 771-781, Mar. 1999.

[37] J. Boutros, N. Gresset, L. Brunel, M. Fossorier, Soft-input Soft-output Lattice Sphere Decoder for Linear Channels," *IEEE GLOBECOM'03*, San Fransisco, California, USA, Dec. 2003.

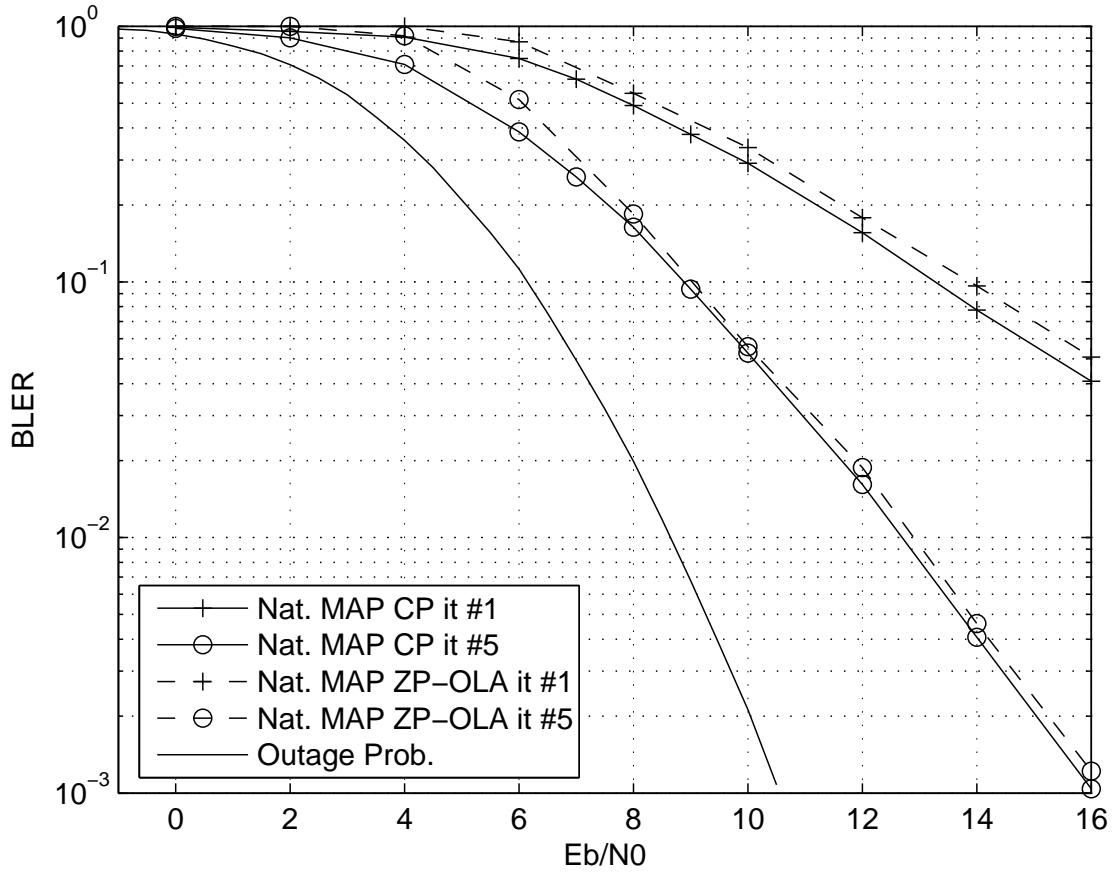[38] M. Sellathurai, S. Haykin, "Turbo-BLAST: Performance Evaluation in Correlated Rayleigh-Fading Environment," *IEEE Journal on selected areas in com.*, vol. 21, no. 3, Apr. 2003.

Fig. 1. Block-static System, 2×2 EXP3, η=6 bpcu, Nat. MAP turbo equalizer
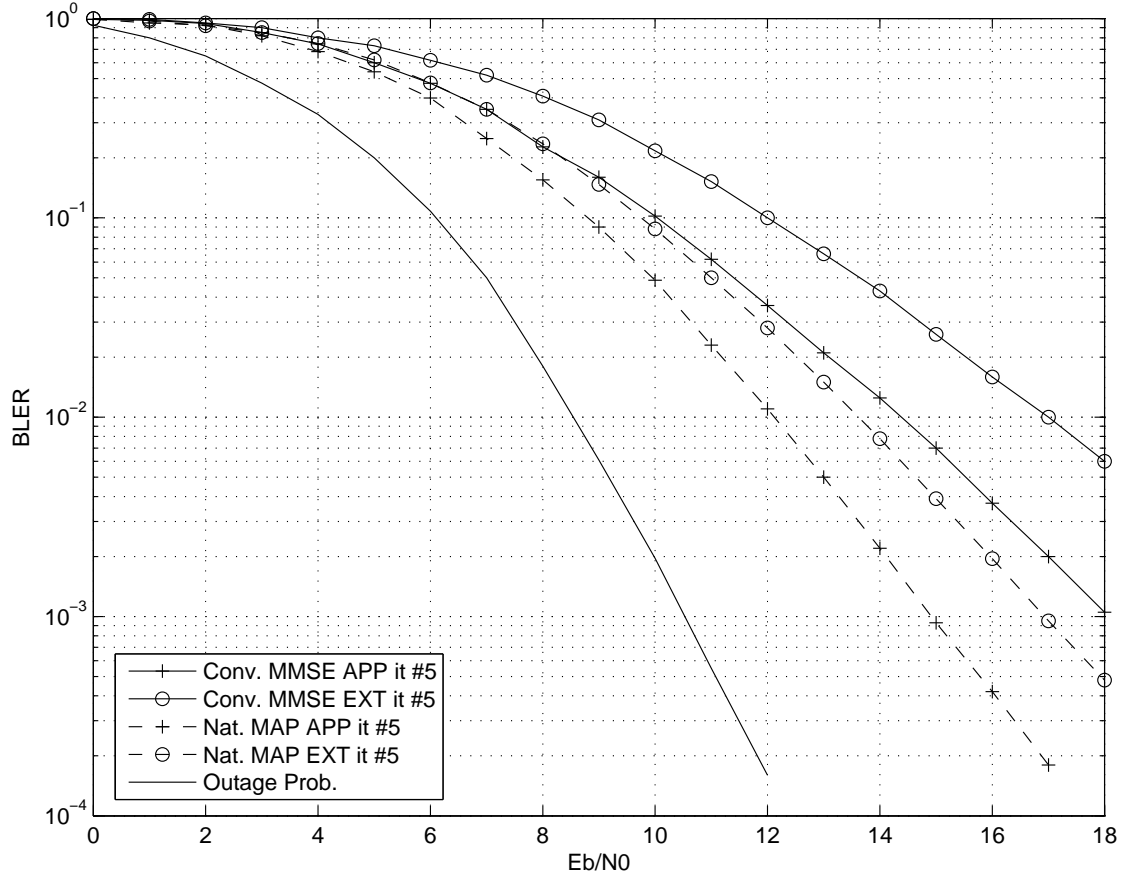
Fig. 2.   Block-static System 2×2 EXP3, η=6 bpcu, Conv. MMSE vs. Nat. MAP turbo equalizer
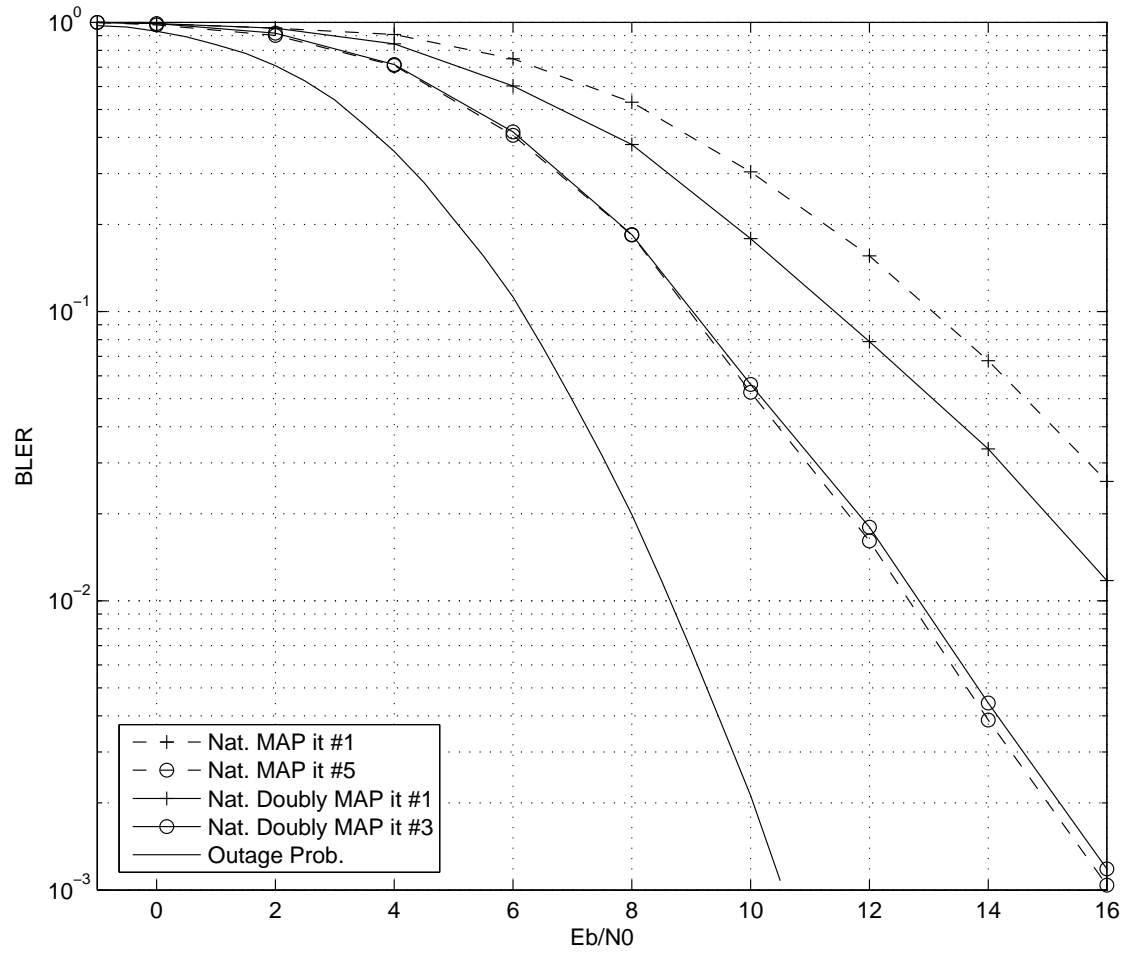
Fig. 3. Block-static System 2×2 EXP3, η=6 bpcu, Nat. MAP vs. Nat. Doubly MAP turbo equalizer

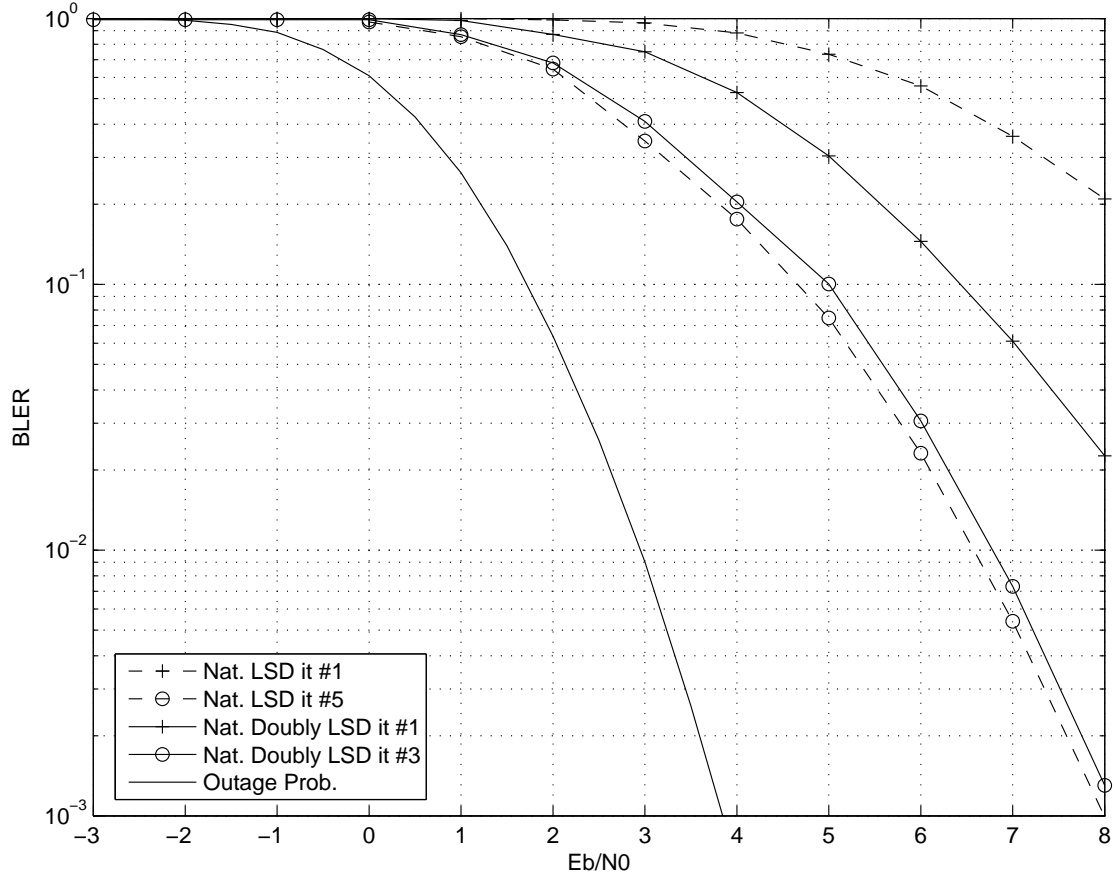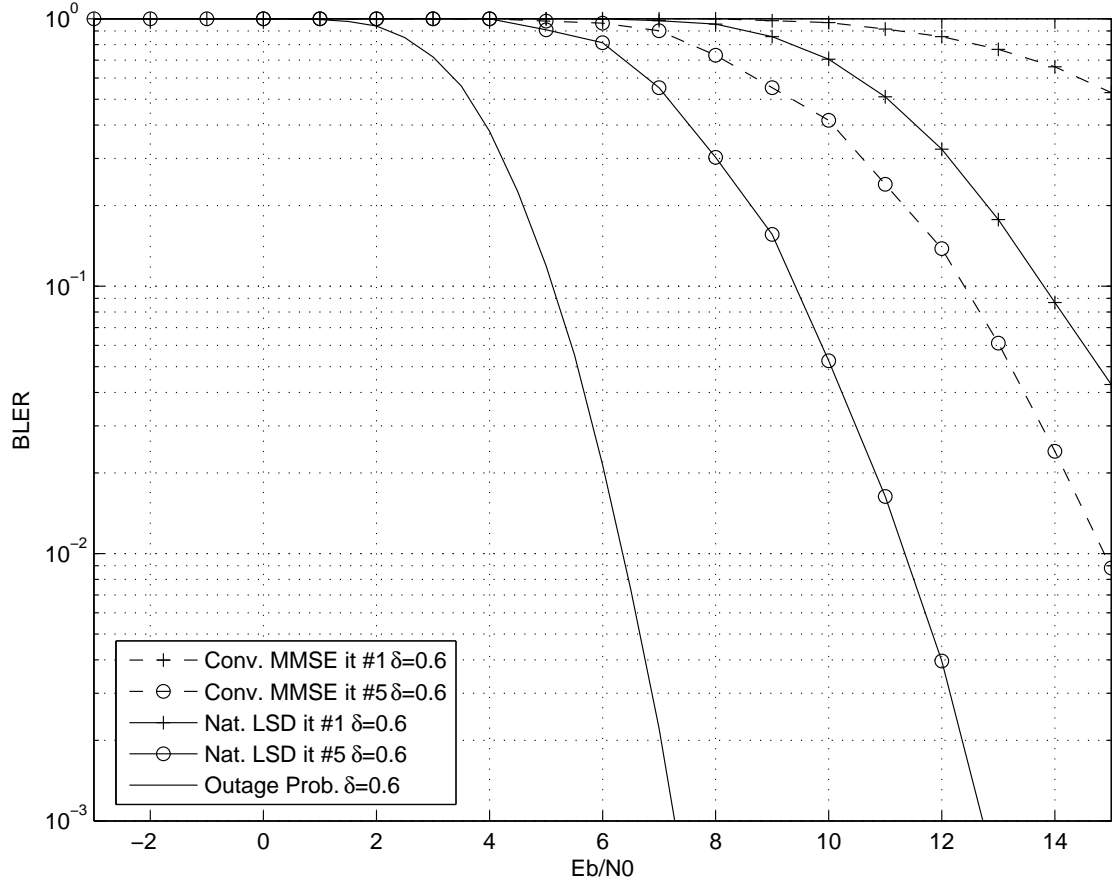Fig. 4. Block-static System 4×4 EXP3 η=12 bpcu, Nat. LSD vs. Nat. Doubly LSD turbo equalizer

Fig. 5.   Block-static System, 4×4 EXP3, $\delta = 0.6$, η=12 bpcu, Conv. MMSE vs. Nat. LSD turbo equalizer
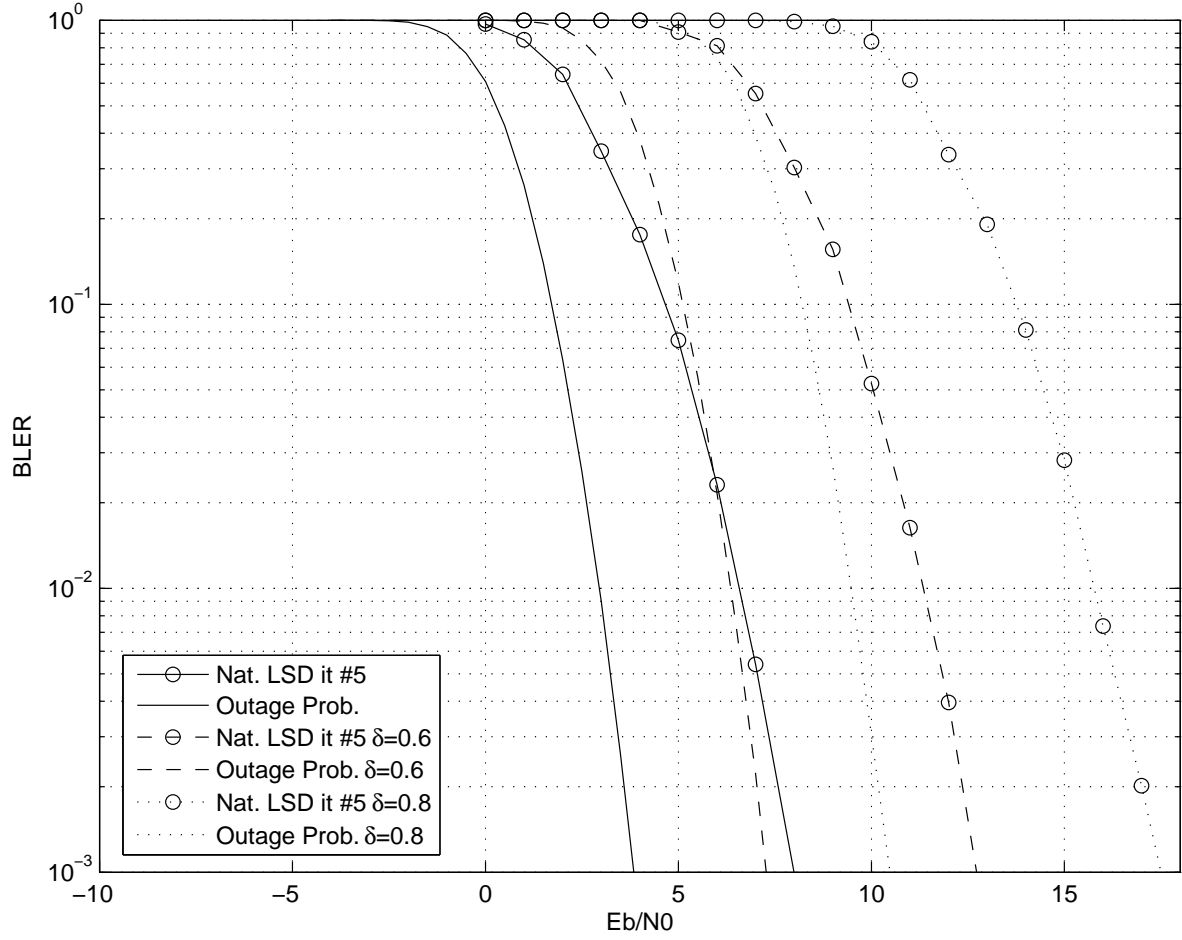
Fig. 6. Block-static System 4×4 EXP3 η=12 bits p.c.u, $\delta = 0.6$ or $\delta = 0.8$, Nat. LSD turbo equalizer vs. Outage Prob.
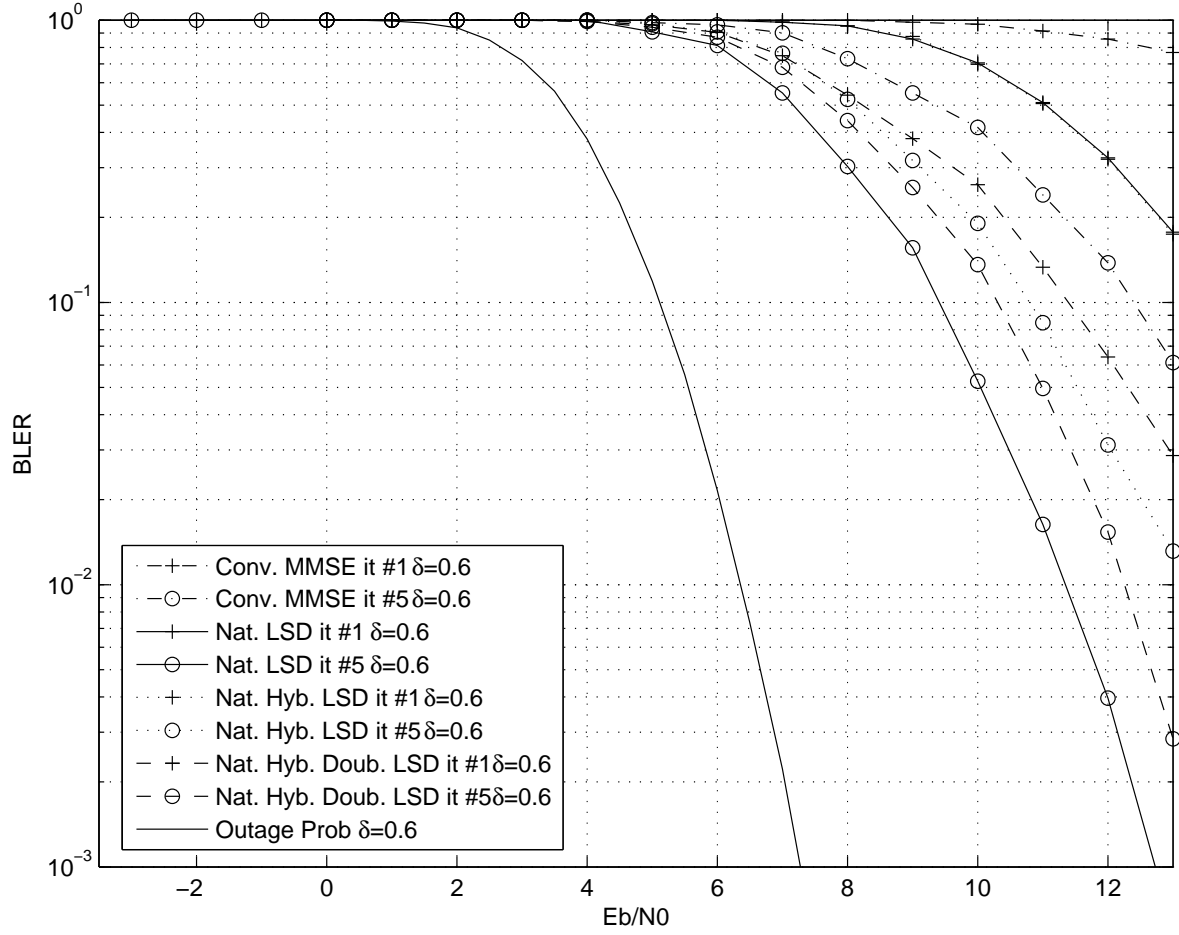
Fig. 7. Block-static System 4×4 EXP3 η=12 bits p.c.u, $\delta = 0.6$, Conv. MMSE, Nat. LSD, Nat. Hybrid LSD, Nat. Hybrid Doubly LSD turbo equalizers